PHYSICAL REVIEW B VOLUME 47, NUMBER 16 15 APRIL 1993-II

Car-Parrinello molecular dynamics with Vanderbilt ultrasoft pseudopotentials

Kari Laasonen*
Institut Romand de Recherche Numérique en Physique des Matériaux (IRRMA), PHB-Ecublens, CH-1015 Lausanne, Switzerland

Alfredo Pasquarello
AT&T Bell Laboratories, 600 Mountain Avenue, Murray Hill, New Jersey 07974

Roberto Car
Institut Romand de Recherche Numérique en Physique des Matériaux (IRRMA), PHB-Ecublens, CH-1015 Lausanne, Switzerland
and Department of Condensed Matter Physics, University of Geneva, Geneva CH-1211, Switzerland

Changyol Lee†
Department of Physics, Harvard University, Cambridge, Massachusetts 02138

David Vanderbilt
Department of Physics and Astronomy, Rutgers University, Piscataway, New Jersey 08855-0849
(Received 29 October 1992)

We show how the ultrasoft pseudopotentials which have recently been proposed by Vanderbilt can be implemented efficiently in the context of Car-Parrinello molecular-dynamics simulations. We address the differences with respect to the conventional norm-conserving schemes, identify certain problems which arise, and indicate how these problems can be overcome. This scheme extends the possibility of performing first-principles molecular dynamics to systems including first-row elements and transition metals.

I. INTRODUCTION

Molecular-dynamics (MD) simulations have been widely used in many different fields, which range from physical chemistry to solid-state physics, to study the microscopic behavior of temperature- and time-dependent phenomena.[1] A great deal of work has been carried out using classical potentials to account for the interactions between atoms. The main drawback of these interaction potentials is that they are usually derived semiempirically from particular bonding situations, and can fail to give an appropriate description when the chemical environment is changed. Because of this transferability problem, it is sometimes desirable to have a MD scheme in which the variations of the electronic structure are accounted for during the simulation. In an important paper, Car and Parrinello[2] proposed a method to perform molecular dynamics in which the electronic structure is described in the density-functional local-density approximation (LDA).[3,4] In this scheme, the ionic forces are determined directly from the electronic structure of the system independently of any empirical parameter, and are therefore highly accurate over a wide range of bonding situations. The Car-Parrinello (CP) method has been successfully applied to a large variety of systems providing detailed information on electronic as well as structural properties.

In spite of the generality of the underlying idea, the Car-Parrinello method has primarily been applied in its original version, i.e., using plane-wave basis sets with periodic boundary conditions in conjunction with pseudopotentials (PP's). There are many advantages of such a basis set. The mathematical formulation is particularly simple. The basis set is independent of the ionic positions, giving an unbiased uniform description of the simulation cell and preventing undesirable Pulay terms[5] from appearing in the calculation of the ionic forces. Plane waves easily allow the use of fast Fourier transforms (FFT's) to transfer quantities from real space to Fourier space and vice versa. Another advantage is the possibility of testing the accuracy of the results by increasing the energy cutoff, which defines the highest kinetic energy of the plane waves in the basis set.

The treatment of the electronic structure causes a considerable increase in the computational effort, such that the size of the system which can be afforded is generally much smaller than for classical simulations. The number of plane waves depends on the size of the system and on the energy cutoff required for a sufficiently accurate description of the electronic structure. This energy cutoff is a property of the PP, and can sometimes affect the feasibility of a CP simulation.

In the original CP version norm-conserving PP's (Refs. 6 and 7) have been used in their fully separable

form.[8] In such a PP scheme, the pseudo-wave-function matches the all-electron wave function beyond a cutoff radius which defines the core region. Within the core region, the pseudo-wave-function has no nodes and is related to the all-electron wave function by the norm-conserving condition which ensures that both wave functions carry the same charge. In the spirit of reducing the energy cutoff, several improvements have been proposed.[9–12] However, despite these improvements, the energy cutoff needed to describe the localized valence orbitals of first-row elements or transitions metals is still frequently too high to allow MD simulations of extended systems.

Recently, Vanderbilt has proposed a new PP scheme in which the norm-conserving condition has been relaxed.[13] In this scheme, the pseudo-wave-functions are allowed to be as soft as possible within the core region, yielding a dramatic reduction of the cutoff energy required to describe them. Technically, this is accomplished by introducing a generalized orthonormality condition, which modifies the conventional approach significantly. In order to recover the full electronic charge, the electron density given by the squared moduli of the wave functions is augmented in the core regions. Thus, the electron density can be subdivided in a smooth part extending throughout the unit cell, and a hard part localized in the core regions. Note that the augmented part appears only in the electron density; this distinguishes the current scheme from others, such as the linearized augmented plane wave (LAPW), in which similar ideas have been applied to the wave functions.

In this paper we address the consequences of the generalized orthonormality condition in the context of Car-Parrinello simulations. The calculations are affected in several ways. First, a new term appears in the Kohn-Sham equations which is dependent on the wave functions and must thus be updated at every time step. Second, the orthonormality condition depends upon the ionic positions. As a consequence, the manner in which this condition is imposed during the ionic motion and the expressions for the ionic forces are substantially modified with respect to the norm-conserving case. Finally, the hard contribution to the electron density must be accounted for without losing the advantage of the low cutoff energy required for the wave functions. In some cases this problem can be ameliorated by a careful generation of a pseudodensity to represent the hard contribution. Otherwise it can be solved using a real-space approach which takes advantage of the fact that the augmented parts of the electron density are localized. We will show that, in spite of the more complex formulation, the present scheme is well suited to handle extended systems containing first-row elements or transition metals.

The paper is organized as follows. In Sec. II we recall the general properties of the Vanderbilt ultrasoft PP scheme. In Sec. III we implement the PP in a Car-Parrinello molecular-dynamics scheme, addressing various consequences of the generalized orthonormality condition. Section IV explains how the implementation is divided between real and reciprocal space. We give a brief summary in Sec. V of various applications that the method already has allowed, and conclude in Sec. VI with a discussion of perspectives and future directions. The Appendix contains an alternative derivation of the constraint contribution to the ionic forces. Although the method has never been described in full, various accounts of specific applications have been presented elsewhere.[14–16]

II. VANDERBILT'S ULTRASOFT PSEUDOPOTENTIAL SCHEME

A. Kohn-Sham equations

In Vanderbilt's ultrasoft PP scheme,[13] the total energy of N_v valence electrons, described by the wave functions ϕ_i, is given by

$$\begin{aligned} E_{\rm tot}[\{\phi_i\},\{\mathbf{R}_I\}] = & \sum_i \langle\phi_i| -\nabla^2 + V_{\rm NL}|\phi_i\rangle \\ & + \tfrac{1}{2}\int\int d\mathbf{r}\, d\mathbf{r}' \frac{n(\mathbf{r})n(\mathbf{r}')}{|\mathbf{r}-\mathbf{r}'|} \\ & + E_{\rm xc}[n] + \int d\mathbf{r}\, V_{\rm loc}^{\rm ion}(\mathbf{r})n(\mathbf{r}) \\ & + U(\{\mathbf{R}_I\}) \ , \end{aligned} \tag{1}$$

where $n(\mathbf{r})$ is the electron density, $E_{\rm xc}$ is the exchange and correlation energy, and $U(\{\mathbf{R}_I\})$ is the ion-ion interaction energy. The PP contains a local part $V_{\rm loc}^{\rm ion}(\mathbf{r}) = \sum_I V_{\rm loc}^{\rm ion}(|\mathbf{r}-\mathbf{R}_I|)$ (Ref. 17) and a fully nonlocal part given by

$$V_{\rm NL} = \sum_{nm,I} D_{nm}^{(0)} |\beta_n^I\rangle\langle\beta_m^I| \ , \tag{2}$$

where the functions β_n^I as well as the coefficients $D_{nm}^{(0)}$ characterize the PP and differ for different atomic species. In the following we will for simplicity consider only one atomic species. The β_n^I functions are centered on site I, and thus depend on the ionic positions through

$$\beta_n^I(\mathbf{r}) = \beta_n(\mathbf{r}-\mathbf{R}_I) \ . \tag{3}$$

Here β_n is an angular momentum eigenfunction in the angular variables, times a radial function which vanishes outside the core region; the indices n and m in Eq. (2) run over the total number N_β of such functions. In the ultrasoft PP case, often two reference energies, and therefore two radial functions, are required for each included angular momentum channel. This leads to a number N_β which is generally twice as large as for a corresponding Kleinman-Bylander[8] norm-conserving PP.

The electron density in Eq. (1) is given by

$$n(\mathbf{r}) = \sum_i \Big[\, |\phi_i(\mathbf{r})|^2 + \sum_{nm,I} Q_{nm}^I(\mathbf{r}) \langle\phi_i|\beta_n^I\rangle\langle\beta_m^I|\phi_i\rangle \,\Big] \ , \tag{4}$$

where the augmentation functions $Q_{nm}^I(\mathbf{r}) = Q_{nm}(\mathbf{r}-\mathbf{R}_I)$ are also provided by the PP and are strictly localized in the core regions. Thus, while the electron density in Eq. (4) is still quadratic in the wave functions, it is now separated into a *soft* delocalized contribution given by the squared moduli of the wave functions, and a new *hard*

contribution localized at the cores. The ultrasoft PP is fully determined by the quantities $V_{\rm loc}^{\rm ion}(\mathbf{r})$, $D_{nm}^{(0)}$, $Q_{nm}(\mathbf{r})$, and $\beta_n(\mathbf{r})$. The algorithm used to generate these quantities is described in Ref. 13 and is briefly reviewed in Sec. II B.

The relaxation of the norm-conserving condition is achieved by introducing a generalized orthonormality condition

$$\langle\phi_i|\, S(\{\mathbf{R}_I\})\,|\phi_j\rangle = \delta_{ij}\ , \tag{5}$$

where S is a Hermitian overlap operator given by

$$S = 1 + \sum_{nm,I} q_{nm}|\beta_n^I\rangle\langle\beta_m^I|\ , \tag{6}$$

and where $q_{nm} = \int d\mathbf{r}\, Q_{nm}(\mathbf{r})$. The orthonormality condition (5) is consistent with the conservation of the charge $\int d\mathbf{r}\, n(\mathbf{r}) = N_v$. Note that the overlap operator S is dependent on the ionic positions through the $|\beta_n^I\rangle$, Eq. (3).

The ground-state orbitals ϕ_i are those which minimize the total energy (1) under condition (5),

$$\frac{\delta E_{\rm tot}}{\delta\phi_i^*(\mathbf{r})} = \epsilon_i\, S\phi_i(\mathbf{r})\ , \tag{7}$$

where ϵ_i have been introduced as Lagrange multipliers. Because of the fact that the augmentation part of the charge density depends on the wave functions,

$$\frac{\delta n(\mathbf{r}')}{\delta\phi_i^*(\mathbf{r})} = \phi_i(\mathbf{r}')\delta(\mathbf{r}'-\mathbf{r}) + \sum_{nm,I} Q_{nm}^I(\mathbf{r}')\beta_n^I(\mathbf{r})\langle\beta_m^I|\phi_i\rangle\ , \tag{8}$$

additional terms appear in the Kohn-Sham equations from the density-dependent terms in the total energy (1). As an example, we consider the exchange and correlation energy. Using Eq. (8) we obtain

$$\begin{aligned}\frac{\delta E_{\rm xc}[n]}{\delta\phi_i^*(\mathbf{r})} &= \int d\mathbf{r}'\,\frac{\delta E_{\rm xc}[n]}{\delta n(\mathbf{r}')}\,\frac{\delta n(\mathbf{r}')}{\delta\phi_i^*(\mathbf{r})} \\ &= \mu_{\rm xc}(\mathbf{r})\phi_i(\mathbf{r}) \\ &\quad + \sum_{nm,I}\beta_n^I(\mathbf{r})\langle\beta_m^I|\phi_i\rangle\int d\mathbf{r}'\,\mu_{\rm xc}(\mathbf{r}')Q_{nm}^I(\mathbf{r}')\ ,\end{aligned} \tag{9}$$

where $\mu_{\rm xc}(\mathbf{r}) = \delta E_{\rm xc}[n]/\delta n(\mathbf{r})$. The other terms can be calculated similarly. We obtain

$$H|\phi_i\rangle = \epsilon_i\, S|\phi_i\rangle\ , \tag{10}$$

where

$$H = -\nabla^2 + V_{\rm eff} + \sum_{nm,I} D_{nm}^I|\beta_n^I\rangle\langle\beta_m^I|\ . \tag{11}$$

Here $V_{\rm eff}$ is the screened effective local potential,

$$V_{\rm eff}(\mathbf{r}) = \frac{\delta E_{\rm tot}}{\delta n(\mathbf{r})} = V_{\rm loc}^{\rm ion}(\mathbf{r}) + \int d\mathbf{r}'\,\frac{n(\mathbf{r}')}{|\mathbf{r}-\mathbf{r}'|} + \mu_{\rm xc}(\mathbf{r})\ . \tag{12}$$

All the terms arising from the augmented part of the electron density have been grouped together with the nonlocal part of the PP, Eq. (2), by defining new coefficients

$$D_{nm}^I = D_{nm}^{(0)} + \int d\mathbf{r}\, V_{\rm eff}(\mathbf{r})Q_{nm}^I(\mathbf{r})\ . \tag{13}$$

Note, however, that the $D_{nm}^{(0)}$ are just parameters which characterize the PP, whereas the new D_{nm}^I depend on the wave functions through $V_{\rm eff}$, Eq. (12), and have to be updated in the self-consistency procedure. (The treatment given here of the screening of the D matrices is consistent with that of Ref. 14, but differs from, and should be considered to supersede,[18] that of Ref. 13.)

At this stage, the difference with respect to the norm-conserving case resides in the presence of the S operator, the wave-function dependence of the D_{nm}^I, and the fact that the number N_β of β_n^I functions is twice as large. The calculation of the D_{nm}^I, Eq. (13), can be carried out in real space and produces only a modest overhead (see Sec. IV B). The presence of the S operator requires the calculation of the $\langle\beta_n^I|\phi_i\rangle$, which, however, are also needed for the nonlocal PP, and thus do not require any additional computation.

The number of operations needed to calculate one scalar product of this type scales like the number of plane waves $N_{\rm pw}$, and the number of these scalar products is given by $N_{\rm at}N_\beta N_{\rm band}$, where $N_{\rm at}$ is the number of atoms, N_β is the number of β_n functions per atom, and $N_{\rm band}$ is the number of filled states. Since $N_{\rm pw}$ and $N_{\rm band}$ both scale like $N_{\rm at}$, this part scales like $N_{\rm at}^3$, and for large systems it is typically the most time-consuming part. (When also the ionic forces [see Eq. (43)] are calculated, similar scalar products $\langle d\beta_n^I/d\mathbf{R}_I|\phi_i\rangle$ are required, just as in conventional norm-conserving schemes.) Thus, for large systems in which the computational cost related to these scalar products is dominant, one can deduce that the ultrasoft PP scheme becomes advantageous compared to the norm-conserving (NC) scheme when $N_{\rm pw}^{\rm NC} > 2\,N_{\rm pw}$, where we have taken $N_\beta = 2N_\beta^{\rm NC}$. In terms of energy cutoff $E_{\rm c}^{\rm wf}$, the criterion is $E_{\rm c}^{\rm wf,NC} > 1.6\,E_{\rm c}^{\rm wf}$, which is easily satisfied for first-row elements and transition metals.

Very recently King-Smith, Payne, and Lin[23] have shown that it is possible to evaluate the scalar products between the wave functions and the β_n^I functions in real space by taking advantage of the fact that the β_n^I are localized. In this way, this part of the calculation scales like $N_{\rm at}N_{\rm band}$, i.e., like $N_{\rm at}^2$. Although in principle the full calculation would still scale like $N_{\rm at}^3$ because of the orthonormalization procedure, the cost of a previously dominant part of the computation would be considerably reduced, allowing the study of still larger systems.

B. Pseudopotential generation algorithm

In this section we give a concise description of the specific PP generation algorithm introduced in Ref. 13.

As in other PP methods, an all-electron (AE) calculation is first carried out on a free atom in some reference configuration, leading to a screened potential $V_{\rm AE}(r)$. Then for each angular momentum l, a set of reference energies $\epsilon_{l\tau}$ is chosen ($\tau = 1, N_\tau$, typically $1 \le N_\tau \le 3$) to cover the energy range over which good scattering prop-

erties are desired (usually the range of occupied bulk valence states). At each $\epsilon_{l\tau}$, the solution of the Schrödinger equation which is regular at the origin is obtained (for fixed $V_{\rm AE}$),

$$[T + V_{\rm AE}(r)]\,\psi_n(r) = \epsilon_n \psi_n(r) \ . \tag{14}$$

Here n is a composite index, $n = \{lm\tau\}$, and T is the kinetic-energy operator $-\frac{1}{2}\nabla^2$. (The amplitude of ψ_n is assumed to have been fixed in some definite way, e.g., by its value at an arbitrary radius R.) Despite the fact that ψ_n is in general non-normalizable, a bra-ket notation

$$(T + V_{\rm AE} - \epsilon_n)\,|\psi_n\rangle = 0 \tag{15}$$

is adopted as a stand-in for the previous equation. Quantities such as $\langle\psi_n|\psi_n\rangle$ are ill-defined, but the special notation $\langle\psi_n|\psi_m\rangle_R$ will be used to denote the integral of $\psi_n^*(\mathbf{r})\psi_m(\mathbf{r})$ inside the sphere of radius R.

Next, cutoff radii r_{cl} are chosen, and for each ψ_n obtained above, a pseudo-wave-function ϕ_n is constructed, subject only to the constraint that it join smoothly to ψ_n at r_{cl}. No norm-conservation constraint is explicitly imposed. A smooth local potential $V_{\rm loc}(r)$ is also generated in such a way that it matches smoothly to $V_{\rm AE}(r)$ at a cutoff radius $r_c^{\rm loc}$, and a diagnostic radius R is chosen such that R is slightly larger than the maximum of the r_{cl} and $r_c^{\rm loc}$. (R must be outside the r_c's in order that scattering properties calculated there will be meaningful.) Then the orbitals

$$|\chi_n\rangle = (\epsilon_n - T - V_{\rm loc})\,|\phi_n\rangle \tag{16}$$

are formed. These are local (they vanish at and beyond R, where $V_{\rm loc} = V_{\rm AE}$ and $\phi_n = \psi_n$). Thus the matrix of inner products

$$B_{nm} = \langle\phi_n|\chi_m\rangle \tag{17}$$

is well defined.

We now form the quantities $V_{\rm loc}^{\rm ion}$, $D_{nm}^{(0)}$, $Q_{nm}(\mathbf{r})$, and $\beta_n(\mathbf{r})$ needed to specify the PP. $Q_{nm}(\mathbf{r})$ and $\beta_n(\mathbf{r})$ are given by

$$Q_{nm}(r) = \psi_n^*(r)\psi_m(r) - \phi_n^*(r)\phi_m(r) \tag{18}$$

and

$$|\beta_n\rangle = \sum_m (B^{-1})_{mn}|\chi_m\rangle \ . \tag{19}$$

The $|\beta_n\rangle$ are duals to the $|\phi_n\rangle$ and are also local; they form the "projectors" of the nonlocal operators. It follows from Eq. (6) that

$$q_{nm} = \langle\psi_n|\psi_m\rangle_R - \langle\phi_n|\phi_m\rangle_R \ . \tag{20}$$

It is straightforward to verify that the $|\phi_n\rangle$ obey the secular equation

$$\left(T + V_{\rm loc} + \sum_{nm} D_{nm}|\beta_n\rangle\langle\beta_m|\right)|\phi_n\rangle = \epsilon_n\left(1 + \sum_{nm} q_{nm}|\beta_n\rangle\langle\beta_m|\right)|\phi_n\rangle \ , \tag{21}$$

where

$$D_{nm} = B_{nm} + \epsilon_m q_{nm} \ . \tag{22}$$

Finally the quantities $V_{\rm loc}^{\rm ion}(r)$ and $D_{nm}^{(0)}$ are obtained from a "descreening" procedure,

$$V_{\rm loc}^{\rm ion}(r) = V_{\rm loc}(r) - \int d\mathbf{r}'\,\frac{n(\mathbf{r}')}{|\mathbf{r}-\mathbf{r}'|} - \mu_{\rm xc}(r) \ , \tag{23}$$

$$D_{nm}^{(0)} = D_{nm} - \int d\mathbf{r}'\,V_{\rm loc}(\mathbf{r}')n(\mathbf{r}') \ . \tag{24}$$

This PP has been generated in such a way that the following features are reproduced in the reference configuration. (Here we assume that the eigenvalues of the occupied valence orbitals in the reference configuration are included among the chosen $\epsilon_{l\tau}$; this is our standard practice.) (i) The pseudoeigenvalues are equal to the AE ones, and the corresponding orbitals agree exactly outside r_{cl}. (ii) The scattering properties are correct at each $\epsilon_{l\tau}$, in the sense that the logarithmic derivative and its energy derivative match the AE one at that energy.[13] Thus, the transferability, as measured by scattering properties in the reference configuration, can be systematically improved by increasing the number of such energies. (iii) The valence charge density is precisely equal to the AE valence density in the reference configuration (except insofar as it is affected by replacement of the Q_{nm} by pseudodensities as discussed in Sec. II C). This helps improve the transferability with respect to changes in the screening environment.

We illustrate the result of such a procedure for the case of the $3d$ orbital of Cu. In Fig. 1 the all-electron wave function and the pseudo-wave-function obtained with a cutoff radius of $r_{cd} = 2.0$ a.u. are compared. The main advantage of the present scheme over previous ones is that no norm-conservation constraint is imposed during the construction $\psi_n \to \phi_n$ of the pseudo-wave-function. Thus, the construction can be done in such a way as to make the $\phi_n(r)$ as smooth as possible. This is the reason we refer to this scheme as an "ultrasoft" PP scheme.

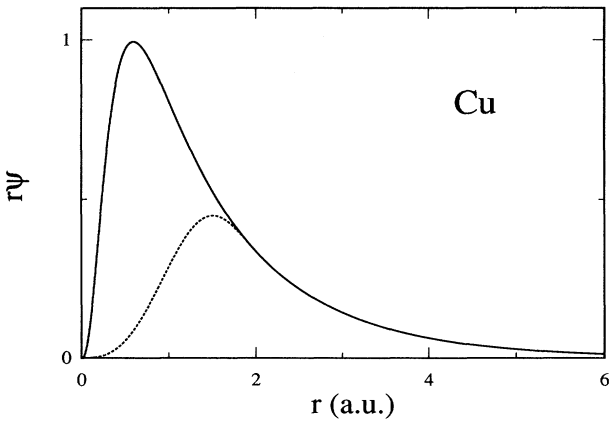

FIG. 1. All-electron (solid) and pseudo (dashed) radial wave functions of the $3d$ orbital of Cu. A cutoff radius of 2 a.u. has been used.

C. Construction of the pseudoelectron charge density

In norm-conserving PP schemes the electron density is defined as in Eq. (4) where only the first term is kept on the right-hand side. Thus, the energy cutoff $E_c^{\rm dens}$ required to describe fully the electron density is four times the energy cutoff $E_c^{\rm wf}$ of the wave functions

$$E_c^{\rm dens} = 4E_c^{\rm wf}. \tag{25}$$

This direct relationship between the cutoff for electron density and wave functions does not hold in the ultrasoft PP scheme because of the presence of the augmentation functions Q_{nm} in the electron density (4). In this scheme, it is therefore appropriate to introduce two independent energy cutoffs: one for the *soft* part of the electron density, $E_c^{\rm soft} = 4E_c^{\rm wf}$, and a second and generally much higher one $E_c^{\rm dens}$ to describe the augmentation functions Q_{nm}.

It is often possible to reduce the charge cutoff $E_c^{\rm dens}$ by replacing the functions Q_{nm} by pseudocounterparts.[13,16] In this construction, the Q_{nm} are modified within an inner core region (defined by $r_{\rm in}$). The charge density described by the pseudo Q_{nm} preserves all the charge moments, so that the electrostatic potential beyond $r_{\rm in}$ remains unchanged. This is achieved by decomposing the Q_{nm} according to angular momentum L as

$$Q_{nm}(\mathbf{r}) = \sum_{LM} c_{LM}^{nm} Y_{LM}(\hat{r}) Q_{nm}^{\rm rad}(r) , \tag{26}$$

where c_{LM}^{nm} are Clebsch-Gordan coefficients, Y_{LM} are spherical harmonics, and $Q_{nm}^{\rm rad}$ gives the all-electron radial dependence of Q_{nm} and is independent of L and M by construction.[13] The number of possible L channels in Eq. (26) is finite because of the fact that a nonlocal PP is required only for the lowest angular momentum channels.

The $Q_{nm}^{\rm rad}$ in Eq. (26) are then replaced by L-dependent counterparts Q_{nm}^{L},

$$Q_{nm}(\mathbf{r}) = \sum_{LM} c_{LM}^{nm} Y_{LM}(\hat{r}) Q_{nm}^{L}(r) , \tag{27}$$

which satisfy the condition that for each L-component the Lth moment of the electron charge density be conserved,

$$\int_0^{r_{\rm in}^L} r^2 dr\, r^L Q_{nm}^L(r) = \int_0^{r_{\rm in}^L} r^2 dr\, r^L Q_{nm}^{\rm rad}(r) , \tag{28}$$

where L-dependent inner cutoff radii $r_{\rm in}^L$ have been introduced. Since the high Fourier components of Q_{nm} are mainly related to the high-L components, it is convenient, for a given cutoff $E_c^{\rm dens}$, to use smaller $r_{\rm in}^L$ for low-L components. In this way, a relatively better description of the lowest moments of the electron charge density is maintained. In Fig. 2 we show the pseudo Q_{nm}^L for $L = 0$, $L = 2$, and $L = 4$ obtained from $Q_{nm}^{\rm rad}$ for the case in which n and m correspond to the same reference energy in the d channel for Cu (corresponding to the wave functions in Fig. 1). The core cutoff radius in this case is 2 a.u., whereas the inner cutoff radii $r_{\rm in}^L$ range from 0.6 a.u. ($L = 0$) to 1.2 a.u. ($L = 4$). With this choice of $r_{\rm in}^L$ it is possible to give a good description

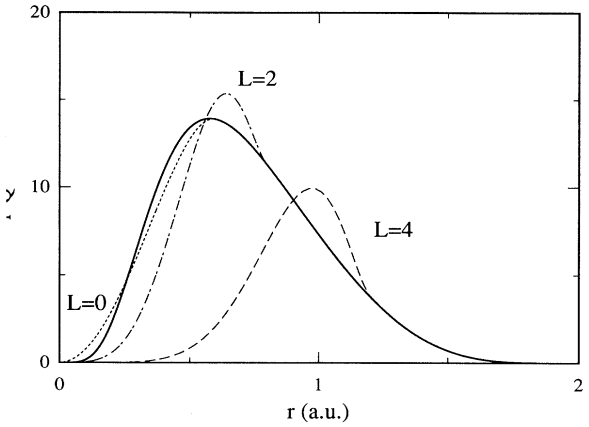

FIG. 2. L-dependent $Q^{\rm rad}(r)$ for the case of the $3d$ orbital of Cu. The original $Q^{\rm rad}$ is given by the solid curve. The pseudo Q^L for $L = 0, 2, 4$ have been obtained with inner cutoff radii $r_{\rm in}^L$ of 0.6, 0.8, and 1.2 a.u., respectively.

of all the Q_{nm}^L using an energy cutoff of about 200 Ry, as can be inferred from Fig. 3 where we show the Fourier transforms of the functions obtained in Fig. 2.

In order to construct optimal pseudo $Q^L(r)$ (where we have dropped the indices n and m), we expand them in polynomials of r inside $r_{\rm in}^L$ as

$$Q^L(r) = r^L \rho_L(r) \qquad \text{when } r < r_{\rm in}^L , \tag{29}$$

where

$$\rho_L(r) = C_1 + C_2 r^2 + C_3 r^4 + \cdots \tag{30}$$

with the number of terms ensuring sufficient smoothness of the polynomial. We want $Q^L(r)$, i.e., $\rho_L(r)$ as smooth as possible. Therefore, following lines similar to Rappe *et al.*,[11] we insist that the Fourier coefficients above a certain cutoff wave vector G_c should be as small as possible. Thus, we minimize

$$I = \int_{G_c}^{\infty} G^2 Q_L^2(G)\, dG , \tag{31}$$

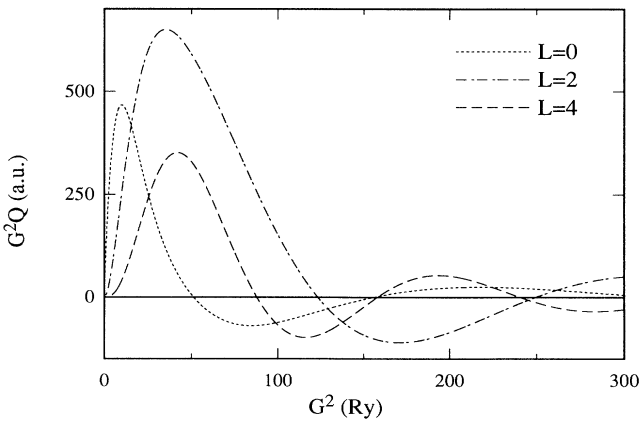

FIG. 3. Fourier transforms of the Q^L given in Fig. 2.

where

$$Q_L(G) = \int_0^\infty r^2 dr\, Q^L(r)\, j_L(Gr) \tag{32}$$

and j_L is the spherical Bessel function of order L. The minimization should be done subject to the constraint (27) and subject to the following continuity requirements:

$$\begin{aligned} \rho(r_{\rm in}^L) &= \rho_{\rm AE}(r_{\rm in}^L)\ , \\ \rho'(r_{\rm in}^L) &= \rho'_{\rm AE}(r_{\rm in}^L)\ , \\ \rho''(r_{\rm in}^L) &= \rho''_{\rm AE}(r_{\rm in}^L)\ , \end{aligned} \tag{33}$$

where the primes indicate radial derivatives. This treatment gives us a very smooth charge density with smooth and continuous first and second derivatives, features which are especially important in the context of gradient-corrected LDA schemes.[19,20] In Fig. 4 we demonstrate the success of this approach for the case of oxygen, specifically for Q_{nm}^L with $L = 0$ and $n, m = 2p$. Figure 4 shows how the Fourier coefficients of the pseudo Q_{nm}^L behave as a function of G when optimally generated according to the above scheme, in comparison to the original Q_{nm}^L, and pseudo Q_{nm}^L generated in a fourth-order polynomial just to give the correct charge and dipole moment and the continuous first derivative of the charge. It is clear that the reciprocal-space convergence is much improved using the present approach.

We have found that in many cases, including that of oxygen, replacement of the Q_{nm} by pseudodensities using the above two refinements (use of L-dependent $r_{\rm in}$ and/or optimally soft construction of the Q^L) allows us to obtain an excellent description of the charge density with $E_{\rm c}^{\rm dens} = E_{\rm c}^{\rm soft}$. In these cases, condition (25) is restored, and the solution of the Kohn-Sham equations (10) can be obtained in the usual way by fast Fourier transforming between a single pair of real-space and reciprocal-space meshes, just as is done with conventional norm-conserving PP's. However, in some cases, and in particular for transition metals such as Cu, even the pseudo Q_{nm} require $E_{\rm c}^{\rm dens} > 4E_{\rm c}^{\rm wf}$. In these cases, the problem of having a large number of plane waves can still be circumvented using the fact that the Q_{nm} are localized in real space. The details of our method for accomplishing this will be discussed later in Sec. IV.

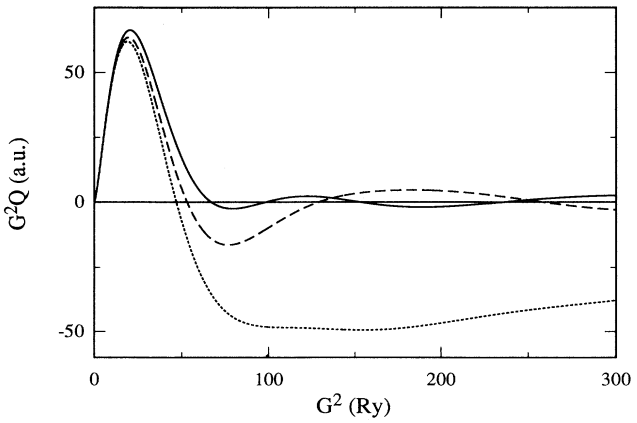

FIG. 4. Fourier components of optimal pseudo (solid), nonoptimal pseudo (dashed), and original (dotted) Q_{nm}^L for oxygen with $L = 0$ and $n, m = 2p$. Vertical scale is arbitrary.

III. MOLECULAR DYNAMICS

A. Lagrangian formulation and ionic forces

Following the CP approach,[2] the electronic wave functions and the ionic coordinates evolve according to a classical Lagrangian

$$\begin{aligned} \mathcal{L} = \mu \sum_i \int d\mathbf{r}\, |\dot\phi_i(\mathbf{r})|^2 + \tfrac{1}{2} \sum_I M_I \dot{\mathbf{R}}_I^2 \\ - E_{\rm tot}(\{\phi_i, \mathbf{R}_I\})\ , \end{aligned} \tag{34}$$

subject to a set of constraints

$$\mathcal{N}_{ij}(\{\phi_i, \mathbf{R}_I\}) = \langle \phi_i | S | \phi_j \rangle - \delta_{ij} = 0\ . \tag{35}$$

Here μ is a fictitious mass parameter for the electronic degrees of freedom, M_I is the mass of the atoms, and $E_{\rm tot}$ and S are as given in Eqs. (1) and (6), respectively. The orthonormality constraints (35) are holonomic, and do not cause energy dissipation during the MD run. They may be incorporated by introducing Lagrange multipliers Λ_{ij} into the Euler equations of motion,

$$\mu \ddot\phi_i = -\frac{\delta E_{\rm tot}}{\delta \phi_i^*} + \sum_j \Lambda_{ij} S \phi_j\ , \tag{36}$$

$$\mathbf{F}_I = M_I \ddot{\mathbf{R}}_I = -\frac{\partial E_{\rm tot}}{\partial \mathbf{R}_I} + \sum_{ij} \Lambda_{ij} \left\langle \phi_i \left| \frac{\partial S}{\partial \mathbf{R}_I} \right| \phi_j \right\rangle . \tag{37}$$

During a MD run, the Lagrange multipliers are to be determined dynamically using the method of Ryckaert *et al.*,[21] as discussed in Sec. III B. For the special case of equilibrium, the vanishing of Eq. (36) reduces (with $\Lambda_{ij} = \epsilon_i \delta_{ij}$) to the electronic Kohn-Sham equations (7) or (10), and the vanishing of Eq. (37) corresponds to the vanishing of the ionic forces $\mathbf{F}_I$. An alternative derivation of the force expression in Eq. (37), particularly applicable to direct minimization approaches, is given in the Appendix.

We now derive explicit expressions for the two terms on the right-hand side of Eq. (37), which correspond to the contributions from the change in the Hamiltonian and from the change in the orthonormality constraints, respectively. The latter contribution appears because of the $\mathbf{R}_I$ dependence of the overlap operator S; note that it is absent in the case of norm-conserving schemes, in which the orthonormality condition does not depend in any way on the ionic positions. The first term on the right-hand side of Eq. (37) must be obtained keeping in mind that the electron density also depends on $\mathbf{R}_I$ through the Q_{nm}^I and β_n^I. Introducing the quantities

$$\rho_{nm}^I = \sum_i \langle \phi_i | \beta_n^I \rangle \langle \beta_m^I | \phi_i \rangle\ , \tag{38}$$

$$\omega_{nm}^I = \sum_{ij} \Lambda_{ij} \langle \phi_j | \beta_n^I \rangle \langle \beta_m^I | \phi_i \rangle\ , \tag{39}$$

with derivatives

$$\frac{\partial \rho^I_{nm}}{\partial \mathbf{R}_I} = \sum_i \left[\left\langle \phi_i \middle| \frac{\partial \beta^I_n}{\partial \mathbf{R}_I} \right\rangle \langle \beta^I_m | \phi_i \rangle + \langle \phi_i | \beta^I_n \rangle \left\langle \frac{\partial \beta^I_m}{\partial \mathbf{R}_I} \middle| \phi_i \right\rangle \right] , \tag{40}$$

$$\frac{\partial \omega^I_{nm}}{\partial \mathbf{R}_I} = \sum_{ij} \Lambda_{ij} \left[\left\langle \phi_j \middle| \frac{\partial \beta^I_n}{\partial \mathbf{R}_I} \right\rangle \langle \beta^I_m | \phi_i \rangle + \langle \phi_j | \beta^I_n \rangle \left\langle \frac{\partial \beta^I_m}{\partial \mathbf{R}_I} \middle| \phi_i \right\rangle \right] , \tag{41}$$

and noting that

$$\frac{\partial n(\mathbf{r})}{\partial \mathbf{R}_I} = \sum_{nm} \left[Q^I_{nm}(\mathbf{r}) \frac{\partial \rho^I_{nm}}{\partial \mathbf{R}_I} + \frac{dQ^I_{nm}(\mathbf{r})}{d\mathbf{R}_I} \rho^I_{nm} \right] , \tag{42}$$

we arrive at the expression

$$\mathbf{F}_I = -\frac{dU}{d\mathbf{R}_I} - \int d\mathbf{r} \, \frac{dV^{\text{ion}}_{\text{loc}}}{d\mathbf{R}_I} n(\mathbf{r}) - \int d\mathbf{r} \, V_{\text{eff}}(\mathbf{r}) \sum_{nm} \frac{dQ^I_{nm}(\mathbf{r})}{d\mathbf{R}_I} \rho^I_{nm} - \sum_{nm} D^I_{nm} \frac{\partial \rho^I_{nm}}{\partial \mathbf{R}_I} + \sum_{nm} q_{nm} \frac{\partial \omega^I_{nm}}{\partial \mathbf{R}_I} , \tag{43}$$

where D^I_{nm} and V_{eff} have been defined in Eqs. (13) and (12), respectively. The last term of Eq. (43) corresponds to the constraint contribution [last term of Eq. (37)]. Note that because the basis set consists of plane waves, the wave functions do not depend on the ionic positions and no additional Pulay-type corrections are needed.[5]

B. Evolution of orthonormality constraints

Here we discuss in some detail the discretization of the equations of motion (36) and (37) using the Verlet algorithm, with special attention to the treatment of the $\mathbf{R}_I$ dependence of the orthonormality constraints. For the electronic wave functions we obtain

$$\phi_i(t+\Delta t) = 2\phi_i(t) - \phi_i(t-\Delta t) - \frac{(\Delta t)^2}{\mu} \left[\frac{\delta E_{\text{tot}}}{\delta \phi^*_i} - \sum_j \Lambda_{ij}(t+\Delta t) \, S(t) \phi_j(t) \right] , \tag{44}$$

where $S(t)$ means that the operator S is evaluated for ionic positions $\mathbf{R}_I(t)$. Similarly for the ionic coordinates,

$$\mathbf{R}_I(t+\Delta t) = 2\mathbf{R}_I(t) - \mathbf{R}_I(t-\Delta t) - \frac{(\Delta t)^2}{M_I} \left[\frac{\partial E_{\text{tot}}}{\partial \mathbf{R}_I} - \sum_{ij} \Lambda_{ij}(t+\Delta t) \left\langle \phi_i(t) \middle| \frac{\partial S(t)}{\partial \mathbf{R}_I} \middle| \phi_j(t) \right\rangle \right] . \tag{45}$$

The orthonormality condition has to be imposed at each time step[21]

$$\langle \phi_i(t+\Delta t) | S(t+\Delta t) | \phi_j(t+\Delta t) \rangle = \delta_{ij} . \tag{46}$$

Fulfilling this constraint leads to the following matrix equation for the Lagrange multipliers $\lambda = \Delta t^2 \Lambda^*(t+\Delta t)/\mu$:

$$A + \lambda B + B^\dagger \lambda^\dagger + \lambda C \lambda^\dagger = 1 , \tag{47}$$

where a dagger indicates the Hermitian conjugate (because of the Hermiticity of S, $\lambda = \lambda^\dagger$) and where

$$\begin{aligned} A_{ij} &= \langle \bar{\phi}_i | S(t+\Delta t) | \bar{\phi}_j \rangle , \\ B_{ij} &= \langle S(t)\phi_i(t) | S(t+\Delta t) | \bar{\phi}_j \rangle , \\ C_{ij} &= \langle S(t)\phi_i(t) | S(t+\Delta t) | S(t)\phi_j(t) \rangle , \end{aligned} \tag{48}$$

with

$$\bar{\phi}_i = 2\phi_i(t) - \phi_i(t-\Delta t) - \frac{(\Delta t)^2}{\mu} \frac{\delta E_{\text{tot}}(t)}{\delta \phi^*_i} . \tag{49}$$

In norm-conserving schemes the identity operator is found in place of S, which leads to a simpler form of Eq. (47) presented in Ref. 22. In the ultrasoft PP case, the solution of Eq. (47) is somewhat problematic because Eq. (45) is not a closed expression for $\mathbf{R}_I(t+\Delta t)$. The problem is that $\Lambda(t+\Delta t)$ appearing in Eq. (45) depends upon $S(t+\Delta t)$ through Eqs. (47)–(49), and thus upon $\mathbf{R}_I(t+\Delta t)$. Consequently, in principle it is necessary to solve iteratively for $\mathbf{R}_I(t+\Delta t)$. We do this by first estimating the new $\Lambda(t+\Delta t)$ using two previous values,

$$\Lambda^{(0)}_{ij}(t+\Delta t) = 2\Lambda_{ij}(t) - \Lambda_{ij}(t-\Delta t), \tag{50}$$

and using this to find the new $\mathbf{R}^{(0)}_I(t+\Delta t)$, which is correct to $O(\Delta t^4)$. Then Eq. (47) is solved (see below) in a similar way as in the norm-conserving case,[22] giving a new set of $\Lambda^{(1)}_{ij}(t+\Delta t)$, with which the whole procedure is repeated, and so on until convergence is achieved. Fortunately, it turns out in practice that the ionic positions are very well determined by Eq. (50), so that the procedure almost always converges on the very first iteration. Thus, the operations described above are generally executed only once per time step.

In order to solve Eq. (47), we generalize the iterative procedure used in Ref. 22 because the unmodified procedure does not always converge. In the norm-conserving case, the matrix B converges to the identity matrix for vanishing Δt. This is not the case in the ultrasoft PP case. However, when the matrix B is decomposed into Hermitian (B_h) and anti-Hermitian (B_a) parts,

$$B = B_h + B_a, \tag{51}$$

it is straightforward to see that B_a vanishes in the limit of small Δt. The first iteration $\lambda^{(0)}$ can now be obtained from

$$\lambda^{(0)} B_h + B_h \lambda^{(0)} = 1 - A \ , \tag{52}$$

where the C-dependent term has been neglected because of higher order in Δt. Equation (52) can be solved exactly introducing the unitary matrix U, which diagonalizes B_h, $U^\dagger B_h U = D$, where $D_{ij} = d_i \delta_{ij}$. The solution to Eq. (47) can be obtained by iterating

$$\lambda^{(n+1)} B_h + B_h \lambda^{(n+1)}$$

$$= 1 - A - \lambda^{(n)} B_a - B_a^\dagger \lambda^{(n)} - \lambda^{(n)} C \lambda^{(n)}, \tag{53}$$

where at every step the new $\lambda^{(n+1)}$ are obtained in the same way as $\lambda^{(0)}$ had been obtained from Eq. (52).

When imposing the orthonormality condition (46), Eqs. (47)–(49) require the calculation of an additional set of scalar products of the type $\langle \beta_n^I | \phi_i \rangle$ as compared to the norm-conserving case. However, the additional computational overhead for these additional products is modest, since the operations of the form $\langle \partial \beta_n^I / \partial \mathbf{R}_I | \phi_i \rangle$ are more numerous.

IV. RECIPROCAL- AND REAL-SPACE IMPLEMENTATION

A. Double-grid technique

As long as the electron density can be described with a cutoff $E_c^{\rm dens} = 4E_c^{\rm wf}$, molecular-dynamics simulations can be performed without further modifications with respect to norm-conserving schemes,[2] except for the use of appropriate forces for electronic (10) and ionic variables (43). As discussed above, this condition is not always satisfied in the ultrasoft PP scheme. In the case of Cu, for example, in which a large part of the charge of the tightly bound d orbitals is incorporated in the Q_{ij}, $E_c^{\rm dens}$ turns out to be significantly higher than $4E_c^{\rm wf}$.[16] Also in the case of first-row elements, such as F,[24] the p electronic states might be so localized that condition (25) cannot be satisfied. In order to permit an optimal choice for $E_c^{\rm wf}$ and $E_c^{\rm dens}$, it is convenient to develop a scheme in which these two parameters can be chosen independently of each other.

In the calculations, fast Fourier transforms (FFT's) are used to transform physical quantities from $\mathbf{G}$ space to $\mathbf{r}$ space and vice versa. Some products are diagonal in $\mathbf{r}$ space, and thus should be calculated in $\mathbf{r}$ space. Products of this type occur twice: $\phi_i^*(\mathbf{r})\phi_i(\mathbf{r})$ in the calculation of the electron density (4), and $V_{\rm eff}(\mathbf{r})\phi_i(\mathbf{r})$ which appears in (10). The FFT grid must contain all plane waves determined by the energy cutoff $E_c^{\rm soft} = 4E_c^{\rm wf}$ in order to fully describe the results of those multiplications. On the other hand, in order to describe the Q_{nm}, a grid determined by the higher cutoff $E_c^{\rm dens}$ is required. A possible solution consists in using a single grid determined by the cutoff $E_c^{\rm dens}$. However, the number of FFT's per time step which have to be performed for the calculation of $\mathbf{r}$-space products scales like the number of electronic states $N_{\rm band}$, whereas only a few FFT's (independent of $N_{\rm band}$) per time step involve the electron density. We have therefore introduced two different FFT grids,[16] a coarse and a dense grid, determined by cutoffs $E_c^{\rm soft}$ and $E_c^{\rm dens}$, respectively. In this way, the FFT's for the $\mathbf{r}$-space products are calculated on the coarse grid with the same numerical effort required in a norm-conserving scheme when using the same wave-function cutoff $E_c^{\rm wf}$. The numerical cost of the few FFT's on the dense grid is negligible in a simulation of a large system. The connection between the two different grids is established in $\mathbf{G}$ space. All the quantities defined on the coarse grid can be transferred to the denser grid, taking the plane-wave components which are absent on the coarse grid to be vanishing.

We illustrate this technique, following the calculations stepwise. In the actual calculations, the electronic degrees of freedom are the coefficients $\phi_i(\mathbf{G})$ of the plane waves

$$\phi_{j,\mathbf{k}}(\mathbf{r}) = \frac{1}{\sqrt{\Omega}} \sum_{\mathbf{G}}^{\mathbf{G}_c^{\rm wf}} \phi_{j,\mathbf{k}}(\mathbf{G}) e^{-i(\mathbf{k}+\mathbf{G})\cdot\mathbf{r}}, \tag{54}$$

where Ω is the volume of the simulation cell and $\mathbf{G}_c^{\rm wf}$ the largest $\mathbf{G}$ vector compatible with the condition $\frac{1}{2}|\mathbf{k}+\mathbf{G}|^2 < E_c^{\rm wf}$. Due to the large simulation cell the Brillouin zone is often sampled using only the Γ point. An advantage of this choice is that the wave functions can be taken to be real. In the following we will drop the $\mathbf{k}$ index.

The scalar products $\langle \phi_j | \beta_n^I \rangle$ and their spatial derivatives are evaluated in $\mathbf{G}$ space

$$\langle \phi_j | \beta_n^I \rangle = \sum_{\mathbf{G}}^{\mathbf{G}_c^{\rm wf}} \phi_j^*(\mathbf{G}) \beta_n(\mathbf{G}) e^{-i\mathbf{G}\cdot\mathbf{R}_I} \ , \tag{55}$$

$$\left\langle \phi_j \left| \frac{d\beta_n^I}{d\mathbf{R}_I} \right. \right\rangle = -i \sum_{\mathbf{G}}^{\mathbf{G}_c^{\rm wf}} \mathbf{G} \phi_j^*(\mathbf{G}) \beta_n(\mathbf{G}) e^{-i\mathbf{G}\cdot\mathbf{R}_I} \ . \tag{56}$$

The kinetic energy is diagonal in $\mathbf{G}$ space and can also be directly calculated

$$E_{\rm kin} = \tfrac{1}{2} \sum_{i,\mathbf{G}}^{\mathbf{G}_c^{\rm wf}} G^2 |\phi_i(\mathbf{G})|^2 \ . \tag{57}$$

The soft part of the electron density $n_{\rm soft}$, given by the first term on the right-hand side of Eq. (4), is obtained in $\mathbf{r}$ space using FFT's on the coarse grid. Then it is transformed to $\mathbf{G}$ space using a coarse-grid FFT. The electron density is now augmented with the contribution arising from the Q_{nm}^I,

$$n(\mathbf{G}) = n_{\rm soft}(\mathbf{G}) + \sum_{i,nm,I} Q_{mn}^I(\mathbf{G}) \langle \phi_i | \beta_n^I \rangle \langle \beta_m^I | \phi_i \rangle \ . \tag{58}$$

The $\mathbf{G}$ vectors required to describe the augmented part are given by the condition $\frac{1}{2}G^2 < E_c^{\rm dens}$, $\mathbf{G}_c^{\rm dens}$ being

the largest of such vectors. In fact, the Q^I_{mn} are first evaluated in $\mathbf{r}$ space on the dense grid, and then transformed with a dense-grid FFT to $\mathbf{G}$ space to be added to the soft electron density $n_{\rm soft}$ in Eq. (58). The $n(\mathbf{G})$ thus obtained is used to evaluate the contribution to the total energy from the local potential

$$E_{\rm loc} = \sum_{\mathbf{G}}^{\mathbf{G}_c^{\rm dens}} V_{\rm loc}^{\rm ion}(\mathbf{G}) n^*(\mathbf{G}) \tag{59}$$

as well as from the Hartree energy

$$E_H = 2\pi\Omega \sum_{\mathbf{G}\neq 0}^{\mathbf{G}_c^{\rm dens}} \frac{n^*(\mathbf{G}) n(\mathbf{G})}{G^2} . \tag{60}$$

The Ewald summation method has been used to correctly cancel the $\mathbf{G}=0$ component in Eq. (60). The electron density is then transformed to $\mathbf{r}$ space on the dense grid, where the energy $E_{\rm xc}$ and the potential $\mu_{\rm xc}$ are evaluated.

The potential $V_{\rm eff}$, Eq. (12), is needed on the dense grid to calculate quantities such as the D^I_{nm}, Eq. (13), *and* on the coarse grid to calculate $V_{\rm eff}\phi_i$ in the Kohn-Sham equations, Eq. (10). The first two terms of $V_{\rm eff}$ are added in $\mathbf{G}$ space on the dense grid. Then the result is transformed to $\mathbf{r}$ space using a dense-grid FFT, where the previously calculated $\mu_{\rm xc}$ is added. The $V_{\rm eff}$ is now known in $\mathbf{r}$ space on the dense grid where it will be used for the D^I_{nm}. The potential $V_{\rm eff}$ is also needed in $\mathbf{r}$ space on the coarse grid. The connection between the two grids is in $\mathbf{G}$ space: $V_{\rm eff}$ is first transformed to $\mathbf{G}$ space on the dense grid, then transferred to the coarse-grid $\mathbf{G}$ space by truncating components incompatible with $E_c^{\rm soft}$, and then backtransforming to $\mathbf{r}$ space using a coarse-grid FFT.

In this way the dense-grid FFT is used only four times per time step, which is negligible compared to the number of coarse-grid FFT's, which scales as the number of states $N_{\rm band}$.

B. Fourier interpolation scheme

We now focus on the augmentation functions Q_{nm}, which are peculiar to the ultrasoft PP scheme. These functions appear in the calculation of the electron density, Eq. (58), in the integrals which give the D_{nm}'s, Eq. (13), and in similar integrals involving $dQ^I_{nm}/d\mathbf{R}_I$ which appear in the ionic forces, Eq. (43). The Q_{nm} need a high cutoff $E_c^{\rm dens}$ and, if these calculations were carried in $\mathbf{G}$ space on the dense grid, a significant increase in the computational cost would occur. It is therefore important to take advantage of the fact that the Q_{nm} are localized in the core regions. When these integrals are calculated in $\mathbf{r}$ space, the associated computational cost is reduced by the ratio of the volumes of the core region and of the simulation cell Ω. In this way, the computational cost related to this part becomes very modest.

The advantage of working in $\mathbf{G}$ space is that the Q^I_{nm} can easily be evaluated for any atomic position by calculating a simple phase factor (Fourier interpolation),

$$Q^I_{nm}(\mathbf{G}) = Q_{nm}(\mathbf{G}) e^{-i\mathbf{G}\cdot\mathbf{R}_I} . \tag{61}$$

When the energy and the forces are both calculated in $\mathbf{G}$ space, the forces are the analytical derivatives of the expression for the energy, ensuring that the constant of motion (e.g., the energy in the Newtonian dynamics) be conserved during the evolution. The accuracy of such a real-space interpolation is therefore extremely critical to guarantee an accurate and stable molecular-dynamics simulation.

We have been able to combine the advantages of the locality of the Q^I_{nm} and the Fourier interpolation scheme, by introducing a small box for every ion. These boxes are taken to be large enough to contain the core regions, where the Q^I_{nm} are nonvanishing. The FFT grid of the boxes locally coincides in $\mathbf{r}$ space with the dense grid. Generally the Q^I_{nm} are obtained using phase factors similar to (61) to take into account the displacement of the ions within their boxes. But when the ion crosses one of the grid planes, the box is displaced discretely by one grid unit to follow the motion of the ion. The advantage of working with these small boxes is that the energy cutoff of the plane waves associated with the box grid is the same as for the dense grid, whereas the number of plane waves is reduced by the ratio of the volumes of the box and Ω.

In the case of the electron density, Eq. (58), the N_β^2 terms corresponding to the indices n and m are first summed for every ion. Then, the result is transformed to $\mathbf{r}$ space of the box grid using a box-grid FFT, and then transferred to $\mathbf{r}$ space on the dense grid. When these operations have been completed for all the ions, this hard part of the electron density is transformed with a dense-grid FFT to $\mathbf{G}$ space. The integrals involving $V_{\rm eff}$ in the second term of Eq. (13) and the third term of Eq. (43) are performed by transferring $V_{\rm eff}$ from the dense-grid $\mathbf{r}$ space to the box-grid $\mathbf{r}$ space, transforming with box-grid FFT's to $\mathbf{G}$ space, and summing in the box-grid $\mathbf{G}$ space in the same way as in Eqs. (55) and (56). The overall cost of the box-grid FFT's is negligible. Note that the above procedure has a total cost that scales only linearly with the size of the system, instead of quadratically as would be the case if the dense-grid FFT were used to perform the interpolations.

Because of the fact that the calculation is performed in part in the Fourier space of the dense grid (e.g., Hartree energy and potential) and in part in that of the box grid, this method provides ionic forces which are exact derivatives of the total energy only when all the Fourier expansions are perfectly converged. When this is not the case, the discrepancies appear as little jumps in the constant of motion whenever an ion crosses a grid plane. These deviations can easily be eliminated by taking a large enough $E_c^{\rm dens}$. The increase of $E_c^{\rm dens}$ only modestly affects the overall computational cost.

V. APPLICATIONS

To date, the ultrasoft PP's have already been used in several different systems for both first-row elements[14,15,24,25] and transition metals.[16] The pseu-

TABLE I. Transferability tests of Vanderbilt pseudopotential in molecular environment. The equilibrium bond length d, vibrational frequency ω, and binding energy E_{bind} of an oxygen dimer.

Approach	E_c^{wf} (a.u.)	d (a.u.)	ω (cm^{-1})	E_{bind} (eV)
V (r_c=1.8 a.u.)	20	2.52	1690	8.7
	25	2.51	1650	8.8
V (r_c=1.5 a.u.)	20	2.35	1610	9.4
	25	2.36	1650	9.5
	30	2.36	1660	9.5
V (r_c=1.2 a.u.)	20	2.51	1210	9.1
	30	2.33	1600	9.7
	50	2.32	1610	9.6
BHS	40	2.39	1180	9.0
	85	2.30	1500	9.6
	125	2.28	1630	9.8

dopotentials were first tested in the case of small oxygen molecules.[14] We compare the binding energy, equilibrium bond length, and the vibrational frequency for O_2 as calculated with ultrasoft PP's of different cutoff radii r_c and with a Bachelet-Hamann-Schlüter (BHS) PP (Ref. 7) in Table I. As can be inferred from Table I, the results obtained with the two PP's are close, but those obtained with the ultrasoft PP converge at much lower energy cutoffs E_c^{wf}. The possibility of describing oxygen with such low cutoffs has made possible the study of larger systems, such as small water clusters[25] and ice.[15] In the latter case, velocity autocorrelation functions were extracted from MD simulations and used to obtain information about the phonon soft-mode behavior near a structural phase transition in high-pressure phases of ice. These studies also showed that the weak hydrogen bond requires gradient corrections[19,20] to the LDA to be included if an adequate description of structural properties is to be obtained.

Ultrasoft PP's have also been shown to be capable of treating a transition metal such as Cu.[16] In this case, because of the extremely localized nature of the $3d$ orbitals it has been necessary to use the double-grid technique in conjunction with the Fourier interpolation described in Secs. IV A and IV B, respectively. Comparison with fully converged calculations for Cu_2 obtained with norm-conserving PP's (Ref. 26) shows that Cu can be accurately described with E_c^{wf} = 18 Ry and E_c^{dens} = 200 Ry.[16] The relatively low E_c^{wf} and a technique introduced by Blöchl and Parrinello[27] to treat metallic systems have made possible a Car-Parrinello MD simulation of liquid Cu.[16] In the method of Blöchl and Parrinello, two Nosé-Hoover thermostats[28] are introduced which couple separately to the ionic and electronic degrees of freedom. The former is used to keep the system at a constant physical temperature, whereas the latter is used to prevent the electronic degrees of freedom from acquiring too much energy. The liquid has been simulated by 50 atoms in a simple cubic cell at the experimental density. After preparation of the sample in a liquidlike configuration, the system has been allowed to evolve for about 2 ps. In order to illustrate the stability of the MD simulation, we plot in Fig. 5 the total potential energy and the sum of the potential and ionic kinetic energy as a function of time for part of the motion. The horizontal line is the constant of motion[27] and does not appear to drift within less than 0.012 meV/ps, which is negligible on the time scale of the simulation. This simulation has allowed us to extract static and dynamical properties in very good agreement with experiment. For more details, we refer to Ref. 16.

The ultrasoft pseudopotentials are also being applied to several systems in the context of static total-energy and force calculations. For this purpose, a steepest-descents version of the electronic minimization is typically used while the ionic degrees of freedom are held fixed. Applications to such diverse systems as $BaTiO_3$ (Ref. 29) and point defects in ZnSe (Ref. 30) have been

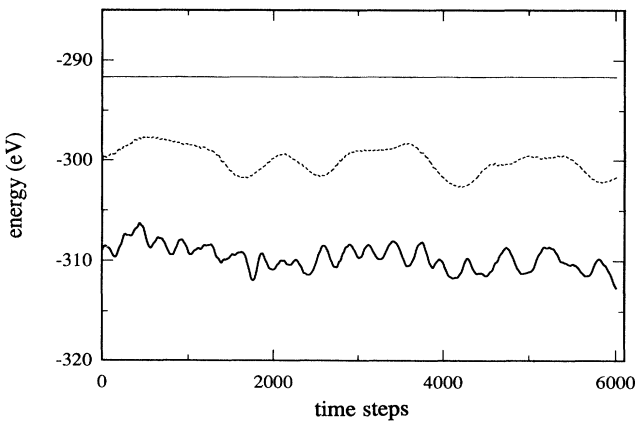

FIG. 5. Total potential energy (solid), sum of potential and ionic kinetic energy (dashed), and constant of motion (thin) for 6000 time steps (1 time step= 0.24 fs) of a Car-Parrinello simulation of liquid Cu.

carried out. In the case of the $BaTiO_3$ calculations particularly, we have found that the ultrasoft pseudopotential scheme has an added advantage because it allows for two shells of the same angular momentum to be included as valence shells. For example, Ba $5s$ and $6s$ shells were both included, as were Ti $3s$ and $4s$ shells, by setting the two reference energies in Eq. (16) equal to the corresponding all-electron eigenvalues. High-quality conventional pseudopotentials containing only a single valence s shell are difficult or impossible to construct for these atoms. In both applications,[29,30] relaxed structures were easily obtained by using the computed ionic forces as a guide.

VI. CONCLUSIONS

Because of the reduced number of plane waves required, the present scheme based on ultrasoft PP's makes it possible to extend first-principles molecular-dynamics simulations to systems containing first-row elements and transition metals, which could not be afforded using norm-conserving pseudopotentials. It should allow the study of relaxation processes in transition-metal molecules or defects, oxidation processes, surface reconstructions, and the properties of liquid and amorphous materials. The present formulation also allows the combined use of ultrasoft pseudopotentials for some of the atoms and standard norm-conserving pseudopotentials for the other ones. Such an approach would be particularly useful for the study of transition-metal or first-row defects in semiconductors.

ACKNOWLEDGMENTS

Two of us (C.L. and D.V.) acknowledge support from NSF Grant No. DMR-91-15342. Three of us (K.L., A.P., and R.C.) acknowledge support from the Swiss National Science Foundation under Grant No. 21-31144.91. We also wish to acknowledge the assistance of R.D. King-Smith and X.-P. Li in the implementation of the method of Eqs. (29)–(33).

APPENDIX: ALTERNATIVE DERIVATION OF IONIC FORCES

Here we briefly give an alternative derivation of the expression for the ionic forces $\mathbf{F}_I$ given in Eqs. (37) or (43) of Sec. III A, and in particular the last term which corresponds to the contribution from the orthonormality constraints. The present derivation makes no reference to the Lagrangian formulation, and is therefore more natural in the context of direct minimization approaches such as conjugate-gradient schemes.

In the main body of this manuscript, we took the point of view that Eq. (1) specifies the total-energy functional even when the ϕ_i depart from the constraints (5). Here we introduce a different generalized functional

$$\widetilde{E}_{\rm tot}(\{\phi_i\},\{\mathbf{R}_I\}) = E_{\rm tot}(\{\overline{\phi}_i(\{\phi_i,\mathbf{R}_I\})\},\{\mathbf{R}_I\}) , \tag{A1}$$

where $E_{\rm tot}$ is as given in Eq. (1), and the $\overline{\phi}_i$ are a new set of S-orthonormal functions

$$|\overline{\phi}_i\rangle = \sum_j (A^{-1/2})_{ji}|\phi_j\rangle \tag{A2}$$

constructed from the ϕ_i via

$$A_{ij} = \langle\phi_i|S|\phi_j\rangle . \tag{A3}$$

We imagine $\overline{\phi}_i = \phi_i$ before the virtual displacement, and calculate the partial derivative $\partial\widetilde{E}_{\rm tot}/\partial\mathbf{R}_I$ holding ϕ_i (but not $\overline{\phi}_i$) constant. While the ϕ_i do not generally continue to satisfy the constraints (5) after the virtual displacement, the $\overline{\phi}_i$ do by construction, and therefore we can associate the above derivative with the physical force,

$$\mathbf{F}_I = -\frac{\partial\widetilde{E}_{\rm tot}}{\partial\mathbf{R}_I} . \tag{A4}$$

We rewrite Eqs. (1) and (4) in the form

$$E_{\rm tot} = \sum_i \langle\overline{\phi}_i|H^{\rm ion}|\overline{\phi}_i\rangle + E_{\rm Hxc}[n] \tag{A5}$$

and

$$n(\mathbf{r}) = \sum_i \langle\overline{\phi}_i|K(\mathbf{r})|\overline{\phi}_i\rangle . \tag{A6}$$

Here

$$H^{\rm ion} = -\nabla^2 + V_{\rm loc}^{\rm ion} + \sum_{nm,I}\left[D_{nm}^{(0)} + \int d\mathbf{r}\, Q_{nm}^I(\mathbf{r})V_{\rm loc}^{\rm ion}(\mathbf{r})\right]|\beta_n^I\rangle\langle\beta_m^I| \tag{A7}$$

and

$$K(\mathbf{r}) = |\mathbf{r}\rangle\langle\mathbf{r}| + \sum_{nm,I} Q_{nm}^I(\mathbf{r})|\beta_n^I\rangle\langle\beta_m^I| . \tag{A8}$$

The notation is essentially that of Ref. 14. The minimization of (A5) leads to the secular equation

$$H|\phi_i\rangle = \sum_j \Lambda_{ij}\, S|\phi_j\rangle , \tag{A9}$$

where $\Lambda_{ij} = \langle\phi_i|H|\phi_j\rangle$, and the screened H is given in Eq. (11).

Using the fact that $A_{ij} = \delta_{ij}$ before the virtual displacement, we find

$$\frac{\partial\overline{\phi}_i(\mathbf{r})}{\partial\mathbf{R}_I} = -\frac{1}{2}\sum_j \left\langle\phi_j\left|\frac{\partial S}{\partial\mathbf{R}_I}\right|\phi_i\right\rangle\phi_j(\mathbf{r}) . \tag{A10}$$

Now the contributions to $\partial E_{\rm tot}/\partial\mathbf{R}_I$ which do not involve the $\mathbf{R}_I$ dependence of the $\overline{\phi}_i$ are

$$\left(\frac{\partial \widetilde{E}_{\rm tot}}{\partial \mathbf{R}_I}\right)_H = \sum_i \left\langle \phi_i \left| \frac{dH^{\rm ion}}{d\mathbf{R}_I} \right| \phi_i \right\rangle + \int d\mathbf{r}\, \frac{\delta \widetilde{E}_{\rm tot}}{\delta n(\mathbf{r})}\, \frac{dn(\mathbf{r})}{d\mathbf{R}_I}$$
$$= \sum_i \left\langle \phi_i \left| \left[\frac{dH^{\rm ion}}{d\mathbf{R}_I} + \int d\mathbf{r}\, \mu_{\rm Hxc}(\mathbf{r})\, \frac{dK(\mathbf{r})}{d\mathbf{R}_I} \right] \right| \phi_i \right\rangle , \tag{A11}$$

while Eq. (A10) leads to additional terms

$$\left(\frac{\partial \widetilde{E}_{\rm tot}}{\partial \mathbf{R}_I}\right)_S = -\sum_{ij} \left\langle \phi_i \left| \frac{\partial S}{\partial \mathbf{R}_I} \right| \phi_j \right\rangle \langle \phi_j | H^{\rm ion} | \phi_i \rangle - \int d\mathbf{r}\, \mu_{\rm Hxc}(\mathbf{r}) \sum_{ij} \left\langle \phi_i \left| \frac{\partial S}{\partial \mathbf{R}_I} \right| \phi_j \right\rangle \langle \phi_j | K(\mathbf{r}) | \phi_i \rangle$$
$$= -\sum_{ij} \left\langle \phi_i \left| \frac{\partial S}{\partial \mathbf{R}_I} \right| \phi_j \right\rangle \Lambda_{ji} . \tag{A12}$$

After a few lines of algebra, it becomes evident that Eq. (A11) generates the second, third, and fourth terms of Eq. (43), while Eq. (A12) corresponds to the last term of Eqs. (37) or (43).

---

*Present address: IBM Research Division, Zürich Research Laboratory, CH-8803 Rüschlikon, Switzerland.
†Present address: Laboratory of Atomic and Solid State Physics, Cornell University, Ithaca, NY 14853-2501.

[1] *Simulations of Liquids and Solids*, edited by G. Ciccotti, D. Frenkel, and I. R. McDonald (North-Holland, Amsterdam, 1986).
[2] R. Car and M. Parrinello, Phys. Rev. Lett. **55**, 2471 (1985).
[3] P. Hohenberg and W. Kohn, Phys. Rev. **136**, B864 (1964).
[4] W. Kohn and L. J. Sham, Phys. Rev. **140**, A1133 (1965).
[5] P. Pulay, Mol. Phys. **17**, 197 (1969); C. Satoko, Phys. Rev. B **30**, 1754 (1984).
[6] D. R. Hamann, M. Schlüter, and C. Chiang, Phys. Rev. Lett. **43**, 1494 (1979).
[7] G. B. Bachelet, D. R. Hamann, and M. Schlüter, Phys. Rev. B **26**, 4199 (1982).
[8] L. Kleinman and D. M. Bylander, Phys. Rev. Lett. **48**, 1425 (1982).
[9] G. Kerker, J. Phys. C **13**, L189 (1980).
[10] D. Vanderbilt, Phys. Rev. B **32**, 8412 (1985).
[11] A. M. Rappe, K. M. Rabe, E. Kaxiras, and J. D. Joannopoulos, Phys. Rev. B **41**, 1227 (1990).
[12] N. Troullier and J. L. Martins, Phys. Rev. B **43**, 1993 (1991).
[13] D. Vanderbilt, Phys. Rev. B **41**, 7892 (1990).
[14] K. Laasonen, R. Car, C. Lee, and D. Vanderbilt, Phys. Rev. B **43**, 6796 (1991).
[15] C. Lee, D. Vanderbilt, K. Laasonen, R. Car, and M. Parrinello, Phys. Rev. Lett. **69**, 462 (1992).
[16] A. Pasquarello, K. Laasonen, R. Car, C. Lee, and D. Vanderbilt, Phys. Rev. Lett. **69**, 1982 (1992).
[17] The interpretation of $V_{\rm loc}^{\rm ion}$ as an atomic or crystalline quantity is to be determined from context.
[18] We thank X. Gonze for first pointing out that the original treatment of the D matrices in Ref. 13 was inconsistent except in the free-atom case.
[19] A. D. Becke, Phys. Rev. A **38**, 3098 (1988).
[20] J. P. Perdew, Phys. Rev. B **33**, 8822 (1986).
[21] J. P. Ryckaert, G. Ciccotti, and H. J. C. Berendsen, J. Comput. Phys. **23**, 327 (1977); G. Ciccotti and J. P. Ryckaert, Comput. Phys. Rep. **4**, 345 (1986).
[22] R. Car and M. Parrinello, *Simple Molecular Systems at Very High Density* (Plenum, New York, 1989), p. 455.
[23] R. D. King-Smith, M. C. Payne, and J. S. Lin, Phys. Rev. B **44**, 13 063 (1991).
[24] A. Satta, A. Pasquarello, and K. Laasonen (unpublished).
[25] K. Laasonen, M. Parrinello, R. Car, C. Lee, and D. Vanderbilt, Chem. Phys. Lett. (to be published).
[26] P. Ballone and G. Galli, Phys. Rev. B **42**, 1112 (1990).
[27] P. Blöchl and M. Parrinello, Phys. Rev. B **45**, 9413 (1992).
[28] S. Nosé, Mol. Phys. **52**, 255 (1984); W. G. Hoover, Phys. Rev. A **31**, 1695 (1985).
[29] R. D. King-Smith and D. Vanderbilt, Ferroelectrics **136**, 85 (1992).
[30] K. W. Kwak, R. D. King-Smith, and D. Vanderbilt, in Proceedings of the 7th Trieste Semiconductor Symposium on Wide-Band-Gap Semiconductors [Physica B (to be published)].